

# Proceedings of the Institution of Mechanical Engineers, Part B: Journal of Engineering Manufacture

<http://pib.sagepub.com/>

---

## Laser milling: Pulse duration effects on surface integrity

P V Petkov, S S Dimov, R M Minev and D T Pham

*Proceedings of the Institution of Mechanical Engineers, Part B: Journal of Engineering Manufacture* 2008 222: 35

DOI: 10.1243/09544054JEM840

The online version of this article can be found at:

<http://pib.sagepub.com/content/222/1/35>

---

Published by:



<http://www.sagepublications.com>

On behalf of:



[Institution of Mechanical Engineers](http://www.institutionofmechanicalengineers.org)

Additional services and information for *Proceedings of the Institution of Mechanical Engineers, Part B: Journal of Engineering Manufacture* can be found at:

**Email Alerts:** <http://pib.sagepub.com/cgi/alerts>

**Subscriptions:** <http://pib.sagepub.com/subscriptions>

**Reprints:** <http://www.sagepub.com/journalsReprints.nav>

**Permissions:** <http://www.sagepub.com/journalsPermissions.nav>

**Citations:** <http://pib.sagepub.com/content/222/1/35.refs.html>

>> [Version of Record](#) - Jan 1, 2008

[What is This?](#)

# Laser milling: pulse duration effects on surface integrity

P V Petkov\*, S S Dimov, R M Minev, and D T Pham

Manufacturing Engineering Centre, Cardiff University, Cardiff, UK

*The manuscript was received on 15 February 2007 and was accepted after revision for publication on 24 July 2007.*

DOI: 10.1243/09544054JEM840

**Abstract:** Laser milling of engineering materials is a viable alternative to conventional methods for machining complex microcomponents. The laser source employed to perform such microstructuring has a direct impact on achievable surface integrity. At the same time, the trade-offs between high removal rates and the resulting surface integrity should be taken into account when selecting the most appropriate ablation regime for performing laser milling. In this paper the effects of pulse duration on surface quality and material microstructure are investigated when ablating a material commonly used for manufacturing microtooling inserts. For both micro- and nanosecond laser regimes, it was estimated that the heat-affected zone on the processed surface is within 50  $\mu\text{m}$ . When performing ultra-short pulsed laser ablation, the effects of heat transfer are not as evident as they are after processing with longer laser pulse durations. Although some heat is dissipated into the bulk when working in pico- and femtosecond regimes it is not sufficient to trigger significant structural changes.

**Keywords:** laser micromachining, micromachining, laser pulse duration

## 1 INTRODUCTION

The laser milling of engineering materials has become a viable alternative to conventional methods for producing tooling inserts for microreplication or for machining microfeatures in components. By applying this technology, material is removed in a layer-by-layer fashion to produce the desired three-dimensional structures. Direct interfaces to three-dimensional computer-aided design (CAD) modelling packages exist to assist in the machining of complex free-form surfaces. Being a non-contact material removal process, some of the main advantages of laser milling are that the process does not suffer from any problems associated with tool breakage, does not require inclusion of collision checking routines in machining programmes, and it is easy to access areas that are very deep in cavities. Also, if ultra-short pulsed lasers are utilized, almost any material can be machined and the thermal load is significantly reduced, resulting in high surface integrity.

Laser radiation can be delivered to the workpiece in an ordered sequence of pulses with a predetermined pulse length (duration) and repetition rate (frequency). This allows the accumulated energy to be released in relatively short time intervals, which is a prerequisite for the formation of extremely high peak powers. Additionally, the laser beam can be focused on a spot with very small dimensions, from submicrometre to 50  $\mu\text{m}$ , which results in a significant energy density (fluence) and intensity (power density) in the spot area. Therefore, an extremely high density can be achieved in the laser-material interaction zone that could not be achieved by any conventional machining technology. This explains the capability of laser milling to process materials that are difficult to machine [1]. In addition, such a high fluence is very important when producing microstructures that require a high surface finish, and hence atom cluster and atomic processing. In particular, to carry out machining at such a scale it is necessary to remove material with units from 1–100 nm to 0.01–1 nm, with a corresponding increase of the specific processing energy from  $10^3 - 10^4$  ( $\text{J}/\text{cm}^3$ ) to  $10^5 - 10^6$  ( $\text{J}/\text{cm}^3$ ) [2], which is attainable with ultra-short pulse laser ablation.

The laser source employed has a direct impact on achievable surface integrity. In recent years a wide

\*Corresponding author: Manufacturing Engineering Centre, Cardiff University, Queen's Building, The Parade, Newport Road, Cardiff CF24 3AA, UK. email: PetkovPV@cf.ac.uk

range of laser sources has become commercially available. Laser pulse durations may vary from microseconds to a few femtoseconds [3]. In this research the effects of pulse duration on surface integrity are investigated when ablating a material commonly used for manufacturing microtooling inserts. In particular, a method for analysing the effects of pulse duration on surface integrity is proposed that takes into account not only the resulting surface roughness after laser milling but also the changes of the material microstructure as a result of the exercised thermal load by different laser sources. Thus, instead of assessing only qualitatively the resulting surface integrity, through this method it is possible to conduct a quantitative analysis of the material grain morphology and thus to judge more precisely the heat penetration depth as a function of pulse duration.

The paper starts with a discussion of the physical phenomena that take place during laser milling with different pulse durations. Then, the set-ups and the method used to carry out this experimental study are outlined and the results of the metallographic and surface profile analyses are provided. Finally, conclusions are made on the effects of pulse duration on the resulting surface integrity.

## 2 MATERIAL REMOVAL MECHANISMS

When pulsed laser machining is performed the actual process of ablating a material takes place within the pulse. Several mechanisms exist for material removal, depending on the laser pulse duration, and some material specific time parameters [4–6]. The following important material-dependent time constants in regard to the substrate material and the laser source are considered:

- $\tau_e$ , the electron cooling time;
- $\tau_i$ , the lattice heating time;
- $\tau_L$ , the laser pulse duration.

As a rule  $\tau_e \ll \tau_i$  and for most materials  $\tau_i$  is in the picosecond range. According to the laser pulse duration, three different ablation regimes can be defined:

- femtosecond:  $\tau_L < \tau_e < \tau_i$ ;
- picosecond:  $\tau_e < \tau_L < \tau_i$ ;
- nanosecond and longer pulses:  $\tau_e < \tau_i < \tau_L$ .

The femtosecond and picosecond ablation mechanisms are similar and are illustrated in Fig. 1.

In these two regimes, the laser radiation is initially absorbed locally in the electron system because the ions are heavier and cannot follow the fast oscillations of the electromagnetic field [7]. The collisions between the energetic electrons and then the electrons and the atomic lattice result in their

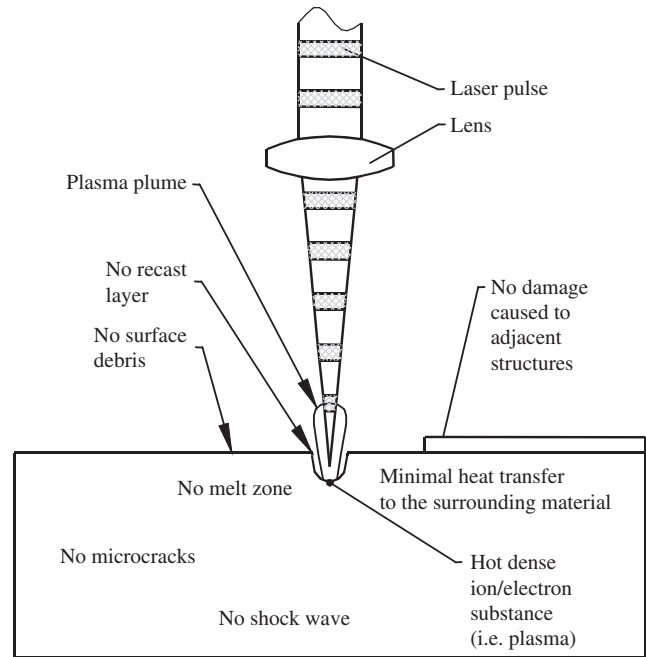


Fig. 1 Femto- and picosecond pulsed laser ablation

thermalization. However, only a small fraction of energy can be transmitted by each electron–lattice collision due to the large mass difference between electrons and ions. Thus, a multiple of electron–phonon relaxation time has to pass to achieve thermodynamic equilibrium between the electron system and the atomic lattice. Therefore, if  $\tau_L$  is much shorter than the time required to reach this thermodynamic equilibrium, the ablation process can be regarded as a direct solid–vapour transition (sublimation), with negligible thermal conduction into the substrate and almost no heat-affected zone (HAZ) [8–11]. In particular, each pulse creates some ‘solid plasma’, a substance consisting of loosely bound ions and electrons, which leaves the substrate after the end of the pulse by expanding in a highly ionized state. The electrons are lighter and are the first to leave the substrate followed by the ions. The latter are all positively charged and repel one another, which facilitates their removal from the substrate. During this expansion the solid plasma takes away most of the energy, and consequently the thermal load on the substrate is very low. In the picosecond regime, in spite of the formation of a molten zone and the existence of some heat conduction, the dominant removal mechanism is still a solid–vapour transition [7].

In general, to perform atom cluster and atomic processing with pulsed lasers,  $\tau_L$  should be shorter than the time necessary to achieve thermodynamic equilibrium between the electron system and the atomic lattice. For example, for metals with strong electron–phonon coupling, such as steel,  $\tau_L$  should

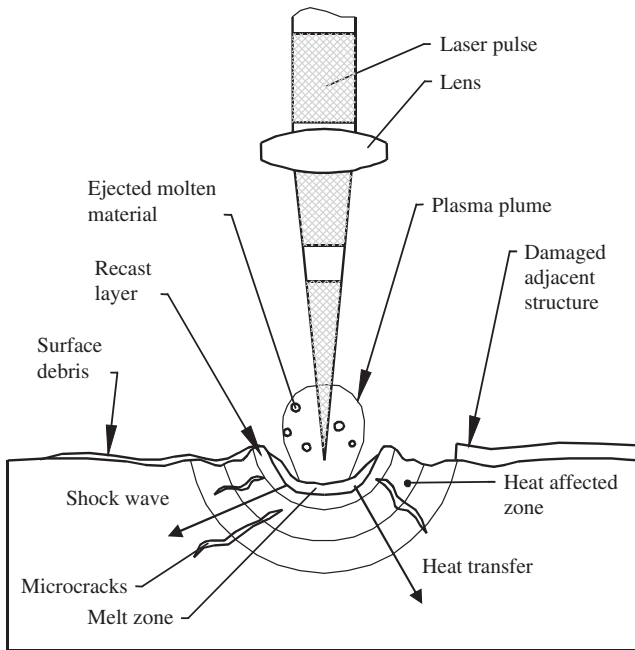


Fig. 2 Nanosecond and longer pulse laser ablation

be in the range from 3 to 5 ps, while for aluminium and copper, materials with weak coupling, it needs to be one or two orders of magnitude higher [7]. A further reduction of  $\tau_L$  would not bring additional benefits in terms of a material machining response. Non-linear effects due to interactions between the ultra-short laser pulse and atmospheric gas in the focal region occur that lead to a wavefront disruption of the beam, profile distortion, and increased beam divergence. In particular, these are the side effects when performing laser ablation in the femtosecond regime [7].

For nanosecond and longer pulses, the process conditions are summarized in Fig. 2. In this case, the absorbed energy from the laser pulse melts the material and heats it to a temperature at which the atoms gain sufficient energy to enter into a gaseous state. There is enough time for a thermal wave to propagate into the material. Evaporation occurs from the liquid state of the material. The molten material is partially ejected from the cavity by the vapour and plasma pressure, but a part of it remains near the surface, held by surface tension forces. After the end of a pulse, the heat quickly dissipates into the bulk of the material and a recast layer is formed [12].

Secondary effects of machining regimes with nanosecond and longer pulses are HAZ, a recast layer, microcracks, shock wave surface damage, and debris from ejected material. Additionally, the vaporized material forms plasma almost at the start of the pulse, and it is sustained throughout it. Due to the plasma shielding effect (absorption and defocusing

of the pulse energy), a higher irradiance (fluence) is required for deeper penetration [12].

In the case of ultra-short pulsed laser ablation, the plasma is formed after the end of the pulse, which means that the shielding effect is avoided. It is important to note that for femto- and picosecond regimes, the fluence should only vary within predefined limits for different materials. Exceeding these limits can lead to undesirable secondary effects [12].

For optimal machining results a proper match between the laser source and the material should be achieved. Generally, higher absorption efficiency leads to a more effective laser milling process. A number of ways exist to increase laser absorptivity, in particular, creating an appropriate surface finish prior to laser milling or applying a suitable surface coating. Laser ablation efficiency can also be increased by performing the laser milling process at elevated temperatures or under water [13].

### 3 EXPERIMENTAL SET-UPS AND METHOD

A series of experiments was conducted to assess the impact of the laser pulse duration on surface integrity of a substrate. Two main effects were studied, in particular changes in material microstructure and surface quality, by carrying out metallographic and surface profile analyses. In particular, to estimate the thermal load exercised on the substrate, the processed areas were analysed for phase transformations and changes in the grain structure.

Four different laser milling systems were employed having femto-, pico-, nano-, and microsecond pulse durations respectively, to ablate a field with dimensions  $1 \times 1$  mm. The characteristics of the laser sources employed in this experimental study are shown in Table 1. The experiments were conducted at four different sites within a day on the same workpiece and included the following.

1. *Familiarization with the material.* The four partner organizations involved in this study did not have experience with the selected material for the trials. Thus, some test features were produced to find the best processing window within the available timeframe. It should be stressed that these may not be the optimal parameters, but the effects on surface integrity of the substrate could be considered representative for performing ablation in these four different regimes.
2. *Machining of a series of  $1 \times 1$  mm fields.* A few test structures were produced on each system by varying laser milling parameters within the identified processing window. However, the available time did not allow the analysis of the machined

**Table 1** Laser sources characteristics

Laser type	Laser source	Laser process parameters	Roughness achieved, Ra ( $\mu\text{m}$ )
A	Femtosecond: laser source SP Hurricane (amplified Ti:sapphire) Wavelength = 800 nm Repeat rate = 5 kHz Pulse = 130 fs Beam diameter = 6 mm Focal distance = 75 mm Spot size = 15 $\mu\text{m}$	Power = 20 mW Scanning speed = 100 mm/min Number of passes = 4 Step = 0.01 mm Fluence = 0.25 J/cm <sup>2</sup>	0.35
B	Picosecond laser source: Stacatto (Lumera) Wavelength = 1064 nm Repeat rate = 50 kHz Pulse = 12 ps Beam diameter = 2 mm Focal distance = 100 mm Spot size = 15 $\mu\text{m}$	Power = 100 mW Scanning speed = 100 mm/s Number of passes = 10 Step = 0.002 mm Fluence = 1.13 J/cm <sup>2</sup>	0.29
C	Nanosecond: CVL MOPA (Oxford lasers) Wavelength = 511 nm Repeat rate = 10 kHz Pulse = 17 ns Beam diameter = 10 mm Focal distance = 100 mm Spot size = 15 $\mu\text{m}$	Power = 10 W Scanning speed = 100 mm/s Number of passes = 10 Step = 0.01 mm Fluence = 2 J/cm <sup>2</sup>	0.86
D	Microsecond: Foba (Lasertech) Wavelength = 1064 nm Repeat rate = 30.5 kHz Pulse = 10 $\mu\text{s}$ Beam diameter = 8 mm Focal distance = 100 mm Spot size = 45 $\mu\text{m}$	Power = 5.2 W Scanning speed = 305 mm/s Number of passes = 10 Step = 0.01 mm Fluence = 1.8 J/cm <sup>2</sup>	2.18

**Table 2** Material properties of BH13

C	Si	Mn	Cr	Mo	V
0.38%	1.00%	0.40%	5.00%	1.30%	1.00%
At temperature					
Physical properties	200 °C	400 °C	600 °C		
Density (kg/dm <sup>3</sup> )	7.75	7.70	7.65		
Coefficient of thermal expansion (per °C from 0 °C)	11.9 × 10 <sup>-6</sup>	12.4 × 10 <sup>-6</sup>	12.8 × 10 <sup>-6</sup>		
Thermal conductivity (cal/cm .s °C)	60.0 × 10 <sup>-3</sup>	62.4 × 10 <sup>-3</sup>	63.6 × 10 <sup>-3</sup>		
Modulus of elasticity (N/mm <sup>2</sup> )	184 000	175 000	154 000		

surfaces to be carried out immediately after the tests. Therefore, as was already indicated, the obtained surface roughness may not be the best achievable with these four laser sources. For further analysis in this research, the fields with the best surface roughness for each of the four studied ablation regimes were selected.

The experiments were conducted on a BS EN ISO 4957-X40CrMoV5-1 tool steel workpiece (0.35% C, 1% Si, 5% Cr, 1.4% Mo, 1% V). This material was selected because it is commonly used to manufacture tooling inserts for microinjection moulding and

hot embossing, and thus to endure many thermal cycles. The material properties of the X40CrMoV5-1 tool steel are provided in Table 2. The workpiece used in this experimental study was polished before it was processed with the four different laser sources in succession.

After completing the machining, all fields on the workpiece were cleaned in an ultrasonic bath with light degreaser to preserve the topology of the resulting surfaces. The fields were inspected with a white light profiling microscope before dicing the substrate in pieces. Then, for a better edge retention the pieces were embedded in an epoxy-based resin.

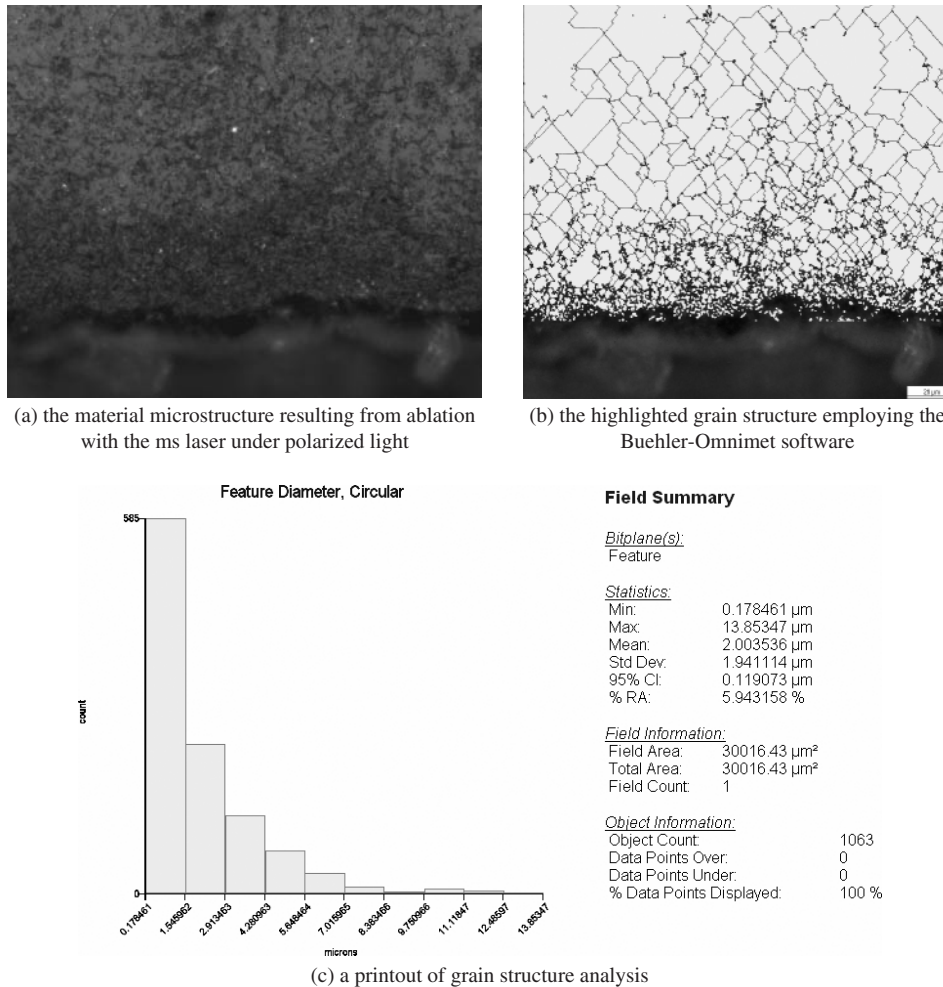


**Fig. 3** Typical results

Finally, the specimens were polished and developed with picral (recommended for structures consisting of ferrite and carbides) and natal (the most common etchant for revealing alpha grain boundaries of Fe, carbon, and alloy steels) reagents in order to analyse the material microstructure. In particular, this was done to highlight the boundaries of the ferrite grains ( $\alpha$ -phase) and carbide sets. An analysis of the material microstructure was carried out employing the Buehler-Omnimet software [14]. In Fig. 3, examples of micrographs depicting the grain structure of the analysed area and a printout showing the number of grains, and their maximum, minimum, and mean diameters, are provided.

The changes in the grain structure were the main criterion for estimating the heat-affected zones. The material microstructure of the workpiece was uniform before performing any processing. After the ablation, a grain refinement was observed in the area surrounding the machined surface. Such changes are the result of the thermal wave propagation into the substrate, which is immediately followed by a quick cooling down at the end of the pulse. In particular, to analyse

the affected regions in this experimental study, they were split into three zones taking into account the extent of these changes. Zone 1 covers the area where the most of the heat was absorbed, and therefore the changes are clearly visible. In zone 2, some changes can still be observed, but at the same time there is a steady decrease of the thermal impact. Finally, in zone 3, the material microstructure can be considered to be the same as in non-processed areas of the substrate.

To make the comparison of microstructure changes easier it was assumed that these three characteristic zones cover the same area in depth for micro- and nanosecond and for pico- and femtosecond ablation regimes respectively. In particular, the three zones were set to be equal for:

- long pulsed lasers (micro- and nanosecond regimes): zone 1 below 15  $\mu\text{m}$  in depth, zone 2 from 15 to 50  $\mu\text{m}$ , and zone 3 above 50  $\mu\text{m}$ ;
- short pulsed lasers (pico- and femtosecond regimes): zone 1 below 10  $\mu\text{m}$ , zone 2 from 10 to 30  $\mu\text{m}$ , and zone 3 above 30  $\mu\text{m}$ .

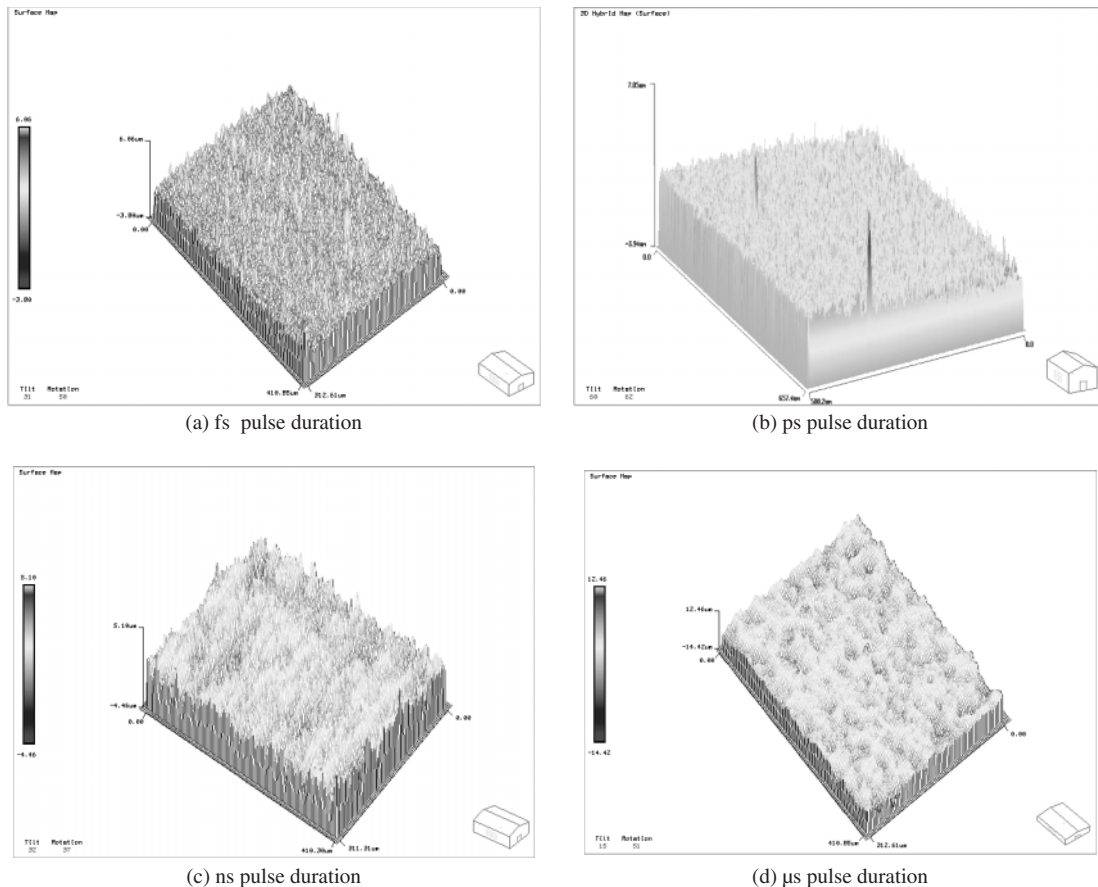


Fig. 4 Three-dimensional surface maps

A quantitative assessment of the microstructure changes was carried out by calculating the number of grains in each zone and their maximum, minimum, and mean diameters with the Buehler–Omnimet software.

## 4 RESULTS

### 4.1 Surface roughness

The surface maps of fields laser milled with different pulse durations were studied in order to understand the effects of the four ablation mechanisms on the resulting surface roughness. As was mentioned in section 3, the fields with the best surface roughness for each of the four studied ablation regimes were selected for further analysis. In Fig. 4, the three-dimensional surface maps of the four studied fields are presented. In addition, surface profiles were created to analyse the effects of pulse duration on the resulting surface topography. They are shown in Fig. 5.

All roughness measurements were taken using a white light profiling microscope. The size of the scanned areas was chosen according to ISO 4288:1996

and ISO 11562:1996 [15]. The parameter used to evaluate the surface roughness was the arithmetic mean roughness ( $R_a$ ) because relative heights in microtopographies are more representative, especially when measuring flat surfaces.

In Fig. 6, the surface profiles of the fields machined with the ps and fs laser sources are superimposed for direct comparison.

### 4.2 Material microstructure

Micrographic pictures were obtained in polarized light in order to enhance the appearance of the crystallographically identical ferrite grains. The area and equivalent circular diameter of each individual grain were calculated using the Buehler–Omnimet software, as was explained in section 3. Based on these data, it was possible to estimate the average grain sizes, and thus to have a quantitative measure for assessing the thermal effects on the processed surfaces, and ultimately to judge the thermal load exercised on the substrate in each ablation regime. A qualitative analysis of the resulting grain structure after performing laser milling with long and short pulsed lasers is provided in Fig. 7.

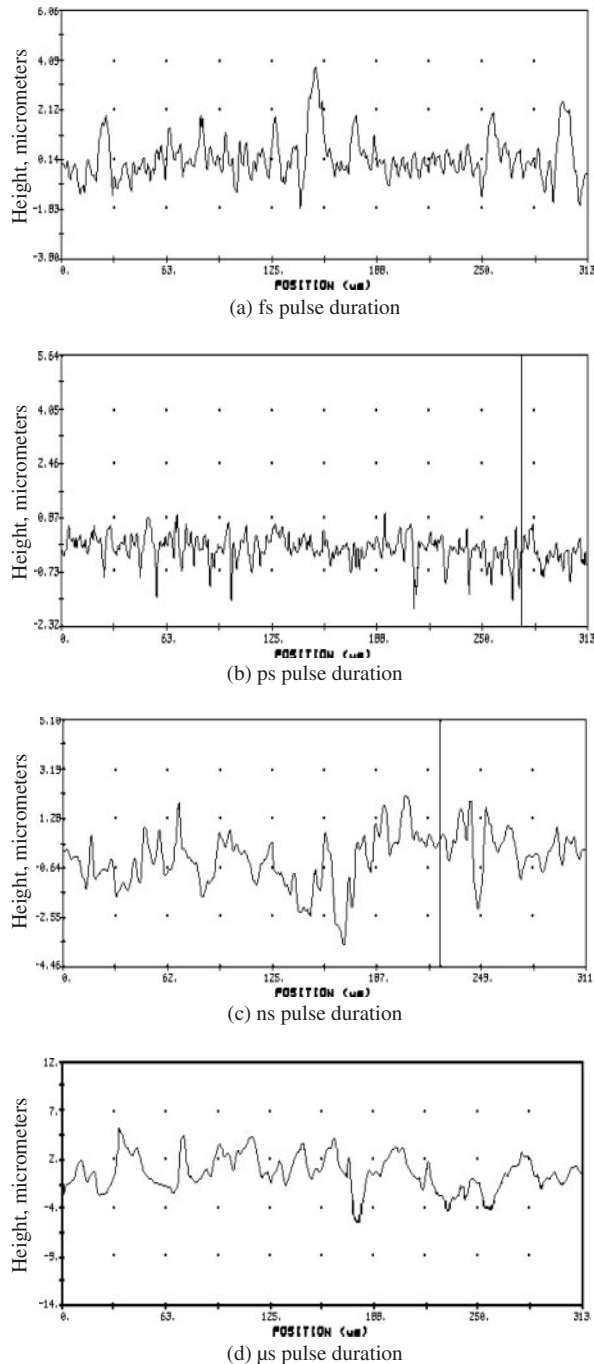


Fig. 5 Surface profiles

The changes of the material microstructures in the three characteristic zones after processing in different ablation regimes can be summarized as follows.

1. *Microsecond pulse duration.* Figure 8(a) shows the studied three characteristic zones. In zone 1 (0–15  $\mu\text{m}$ ) the mean diameter of the grains was estimated to be approximately 1.3  $\mu\text{m}$  and the maximum diameter measured was 7.5  $\mu\text{m}$ . In zone 2 (15–50  $\mu\text{m}$ ) the mean diameter was equal

to 2.5  $\mu\text{m}$  while the maximum diameter was 11.5  $\mu\text{m}$ . Finally, above 50  $\mu\text{m}$  no changes in the grain structure were identified. The mean and maximum diameters were 7.9 and 36  $\mu\text{m}$  respectively, the same as in unprocessed areas on the substrate.

2. *Nanosecond pulse duration.* The three studied zones in the micrograph are shown in Fig. 8(b). In zone 1 the estimated mean diameter of the grains was approximately 1.45  $\mu\text{m}$  while the maximum diameter measured was 9.8  $\mu\text{m}$ . In zone 2, from 15 to 50  $\mu\text{m}$ , the mean and maximum diameters were 2.8 and 15.5  $\mu\text{m}$  respectively. Again, above 50  $\mu\text{m}$  there were no more changes in the grain structure. The mean and maximum diameters were 7.8 and 33  $\mu\text{m}$ .
3. *Picosecond pulse duration.* In Fig. 9(a), a micrograph depicting the three characteristic zones used for analysing the thermal load of short pulsed lasers is provided. The results obtained showed that mean and maximum diameters of the grains in zones 1 and 2 were 2.3 and 4.1  $\mu\text{m}$ , and 9.3 and 21.5  $\mu\text{m}$  correspondingly. No changes in the grain sizes were observed in zone 3, above 30  $\mu\text{m}$ . In particular, the measured mean and maximum diameters were equal to 8.2 and 31  $\mu\text{m}$ , which were the same as those for unprocessed areas of the substrate.
4. *Femtosecond pulse duration.* The analysis of the material microstructure was carried out again by splitting the micrograph in three zones, as shown in Fig. 9(b). In zone 1 the estimated mean diameter of the grains was approximately 1.6  $\mu\text{m}$  while the maximum diameter measured was 8.2  $\mu\text{m}$ . In zone 2, from 10 to 30  $\mu\text{m}$ , the mean and maximum diameters were 4 and 17.5  $\mu\text{m}$  respectively. Again, above 30  $\mu\text{m}$  from the ablated surface there were no changes in the grain structure, and the mean and maximum diameters were 8.2 and 31  $\mu\text{m}$  correspondingly.

## 5 DISCUSSION

### 5.1 Surface roughness

As expected, the roughness of the field processed with the ms laser was the highest, Ra 2.18  $\mu\text{m}$ . The surface profile after machining with the ns laser source was significantly better; in particular, the roughness was reduced to Ra 0.86  $\mu\text{m}$ . However, the results produced working in ps and fs regimes were not expected. Initially, it was anticipated that in these two ablation regimes a shortening of the pulse duration would lead to a better machining response, in particular surface finish. The surface roughness measured on the surface ablated with the fs laser

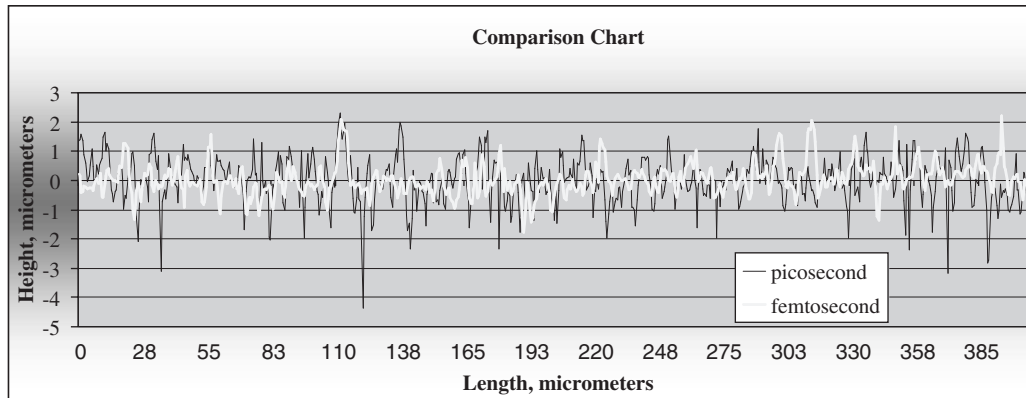
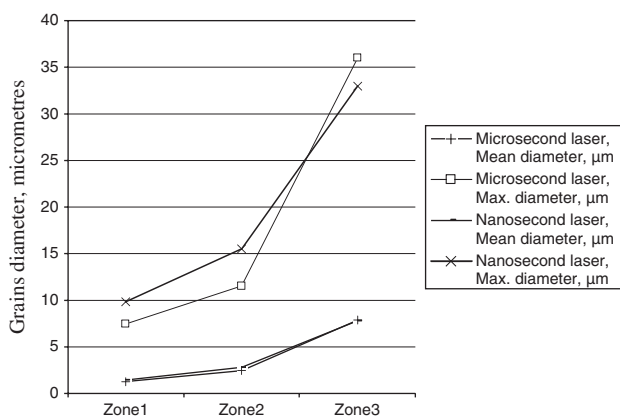
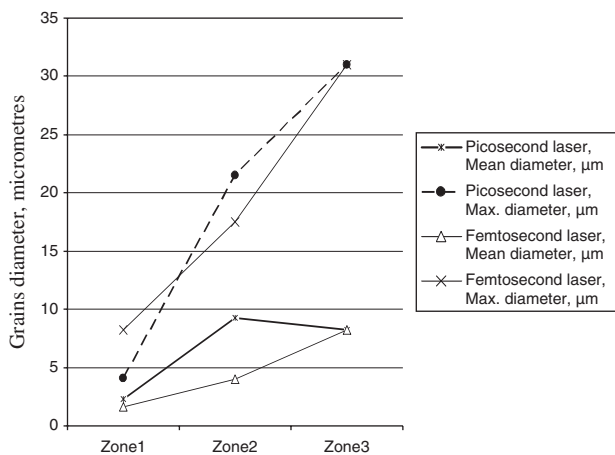


Fig. 6 A direct comparison of the surface profiles of the fields machined with the ps and fs laser sources



(a) The changes of maximum and mean grain diameters in the three studied zones after processing with long pulsed lasers



(b) The changes of maximum and mean grain diameters in the three studied zones after processing with short pulsed lasers

Fig. 7 The changes of maximum and mean grain diameters in the three studied zones

was  $Ra\ 0.35\ \mu\text{m}$  compared to  $Ra\ 0.29\ \mu\text{m}$  achieved with the ps one. This could be explained with non-linear effects that are typical when processing materials at this regime, and also with the specific

machining response of the tooling steel to the selected processing parameters.

## 5.2 Material microstructure

Pulse duration is a major factor affecting the surface integrity of processed areas. In particular, it is important to understand the effects of heat dissipation into the regions nearest to the machined surface. In this research, these effects were studied by analysing the changes in material grain structure, and thus indirectly to make a judgement about the specific thermal load of each ablation regime.

Based on the grain size refinement observed in the areas processed with ms and ns lasers, it was estimated that the temperature in the affected zones 1 and 2 reached more than  $800\text{--}900\text{ }^\circ\text{C}$  before the heat started to dissipate into the substrate. Thus, the temperature was sufficiently high to initiate an austenite ( $\gamma$ ) transformation, which was followed by a  $\gamma \rightarrow \alpha$  transformation with cooling rates much higher than those in a conventional heat treatment. This resulted in the creation of a non-equilibrium microstructure in the material, in particular a higher stress level, smaller  $\alpha$  grain sizes, and carbides precipitated within the  $\alpha$  grains. At the same time the cooling rate was not high enough to initiate a martensite transformation. Martensite transformations were observed only in some areas exposed to extreme conditions, where a significant deterioration of surface integrity was observed together with formation of large torch-like recast zones, as shown in Fig. 10. The microhardness measurements carried out in these areas resulted in values around 550 MHV (see Fig. 10(b)) that are typical for quenched structures. Although, in this case, the martensite structures were an undesired effect, the trials demonstrated that laser systems could be used for performing controlled surface modifications.

As expected, the material microstructures formed after processing with ultra-short laser pulses showed less phase transformations than those created by

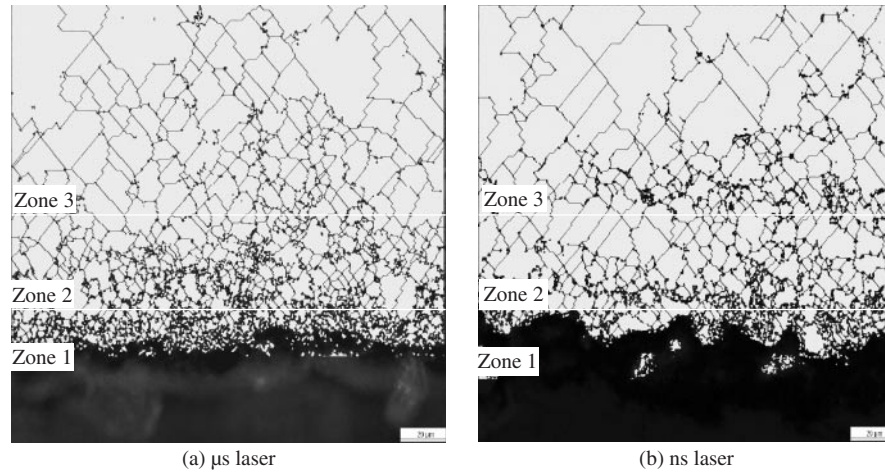


**Fig. 8** A micrograph depicting the three characteristic zones after machining

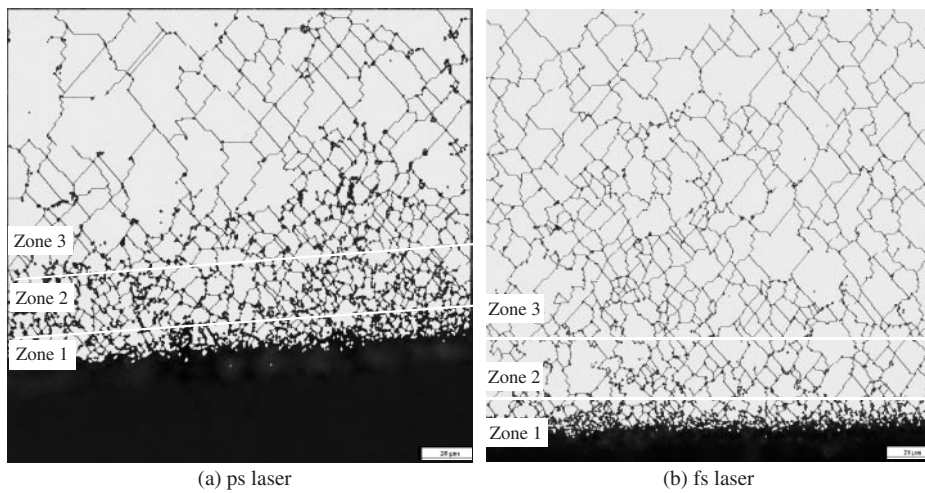


**Fig. 9** A micrograph depicting the three characteristic zones after machining

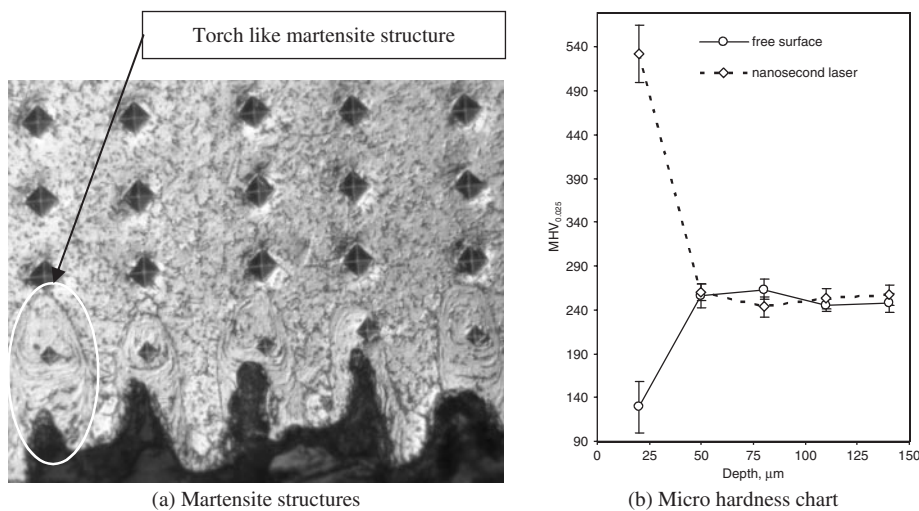


**Fig. 10** Martensite torch-like structures

performing ablation with longer pulses. This can be easily explained with the specific characteristics of these two distinctive ablation regimes. In particular, the material undergoes a direct solid–vapour transition, in the case of ps and fs laser pulses, compared to the solid–melt–vapour transitions when exposed to longer pulses. The melt–vapour proportion determines the amount of heat that is dissipated into the substrate, and eventually causes secondary effects such as microcracks, phase transformations, and grain size changes. As reported by Breitung *et al.* [7], the melt–vapour ratio depends on pulse duration and fluence, and decreases with the reduction of the interaction time. The presence of melt instigates more intensive heat transfer to the substrate, and subsequently a larger HAZ.

In ps and fs laser ablation regimes, the overall energy transfer is very small, and thus the changes of the microstructure are almost negligible. A direct de-sublimation of the atoms occurs and the energy is immediately taken away from the substrate. In spite of that, some changes in material microstructure can still be observed in the micrographs for both ablation regimes. In the case of ps laser ablation they are more evident (see Fig. 9(a)), while for the fs regime if there are any, they are only within 1–2  $\mu\text{m}$  in depth (Fig. 9(b)).

## 6 CONCLUSIONS

In this research, the effects of pulse duration of four different laser sources on surface integrity are investigated. In particular, an attempt is made to assess the impact of four distinctly different laser regimes on surface quality and material microstructure. These are the issues that have to be taken into account when considering the trade-offs between high removal rates and the resulting surface integrity. This is a particular dilemma when selecting the most appropriate ablation regime for performing microstructuring.

During laser milling applying different ablation mechanisms, the material goes through several phase transitions that have a direct impact on surface integrity of the processed area. Thus, the relevant material characteristics are transition energies, such as evaporation energy and melting energy. In addition, thermal conductivity is a key material factor affecting the resulting surface integrity. In particular, this affects the dissipation of the absorbed energy into the bulk of the material and the energy losses, and hence determines the size of the HAZ.

The following generic conclusions could be drawn from this experimental study.

1. For both ms and ns laser milling, it was estimated that the HAZ on the ablated surface was within

50  $\mu\text{m}$ . However, there were some differences in grain size refinements when comparing the resulting microstructures. The melt phase during ms laser processing was bigger, and more heat was transferred into the substrate, leading to formation of a finer grain structure.

2. When performing ultra-short pulsed laser ablation, the effects of heat transfer are not evident, as was the case with longer laser pulse durations. Although some heat is transferred into the bulk, it is not sufficient to trigger significant structural changes. Heat penetration is much smaller and grain refinement is minimal. The effects of pulse duration on the resulting material microstructure are more evident in the micrograph of the field exposed to ps laser ablation than that of the area which underwent processing with fs laser pulses.
3. Due to the ablation mechanism that is in place when applying ultra-short pulses, significant improvements of surface roughness can be achieved by applying ps and fs pulse lasers. In this research, a marginally better surface quality was achieved when performing laser milling with a ps laser source. This could be explained with non-linear effects that are typical for processing materials at fs regimes, and also with the specific machining response of the tooling steel to the selected processing parameters, especially the laser wavelength.

These generic conclusions again underline the existing trade-offs between the resulting surface integrity and removal rates. Therefore, it is required to look for the best compromise when selecting the optimum laser source for each specific application. Taking into account the specific requirements of microtooling applications, in particular as high as possible surface quality and relatively small volumes of material that have to be removed, ultra-short pulsed laser ablation regimes present a viable solution. Furthermore, this research suggests that ps pulse lasers offer some advantages over fs laser sources when they are utilized for machining microcavities in tooling steel. Taking into account that the fluence of the ps laser source is four times higher than that of the fs laser, it can be expected that through further process optimization an even better surface quality could be achieved.

## ACKNOWLEDGEMENTS

The research reported in this paper was funded under the MicroBridge programme supported by the Welsh Assembly Government and the UK Department of Trade and Industry, the EPSRC Programme

'The Cardiff Innovative Manufacturing Research Centre', and the ERDF programme 'Micro Tooling Centre'. Also, it was carried out within the framework of the EC FP6 Networks of Excellence, 'Multi-Material Micro Manufacture (4M): Technologies and Applications' and 'Innovative Production Machines and Systems (I\*PROMS)'. The authors gratefully acknowledge the support given to the Networks by the European Commission.

The authors would like to thank Dr Martyn Knowles and Dr Dimitris Karnakis of Oxford Lasers, Steven Wheeler of Lumera, and Dr Nadeem Rizvi of UK Laser Micromachining Centre for their help in conducting this experimental study.

## REFERENCES

- 1 Lasertech GmbH. Presentations, operating manual, Gildemeister Lasertec GmbH, Tirolerstrasse 85, D 87459 Pfronten, Germany, 1999.
- 2 **Taniguchi, N.** (Ed.) *Nanotechnology: integrated processing systems for ultra-precision and ultra-fine products*, 1996 (Oxford University Press), ISBN 0 19 8562837.
- 3 Fraunhofer Institut Lasertechnik (ILT) website: <http://www.ilt.fhg.de/eng/lasertypen.html>, Last visited: 17.01.06.
- 4 **Shirk, M. D.** and **Molian, P. A.** A review of ultrashort pulsed laser ablation of materials. *J. Laser Applics*, 1998, **10**(1), 18–28.
- 5 **Chichkov, B. N., Momma, C., Nolte, S., von Alvensleben, F., and Tünnemann, A.** Femtosecond, picosecond and nanosecond laser ablation of solids. *Appl. Physics*, 1996, **A63**, 109–115.
- 6 **Momma, C., Nolte, S., Chichkov, B. N., von Alvensleben, F., and Tünnemann, A.** Precise laser ablation with ultrashort pulses. *Appl. Surf. Sci.*, 1997, **109–110**, 15–19.
- 7 **Breitlung, D., Ruf, A., and Dausinger, F.** Fundamental aspects in machining of metals with short and ultrashort laser pulses. *Proc. SPIE*, 2004, **5339**, 49–63.
- 8 **Kautek, W. and Krüger, J.** Femtosecond pulse laser ablation of metallic, semiconducting, ceramic and biological materials. *Proc. SPIE*, 1994, **2207**, 600–610.
- 9 **Preuss, S., Demchuk, A., and Stuke, M.** Sub-picosecond UV laser ablation of metals. *Appl. Physics*, 1995, **A61**, 33–37.
- 10 **von der Linde, D. and Sokolowski-Tinten, K.** The physical mechanisms of short-pulse laser ablation. *Appl. Surf. Sci.*, 2000, **154–155**, 1–10.
- 11 **Leong, K.** Drilling with lasers. *Ind. Laser Solutions for Mfg*, 2000, **15**(9), 39.
- 12 **Kautek, W. and Krüger, J.** Femtosecond pulse laser ablation of metallic, semiconducting, ceramic and biological materials. *Proc. SPIE*, 1994, **2207**, 600–610.
- 13 **Geiger, M., Becker, W., Rebhan, T., Hutfless, J., and Lutz, N.** Increase of efficiency for the XeCl excimer laser ablation of ceramics. *Appl. Surf. Sci.*, 1996, **96–98**, 309–315.
- 14 Buehler–Omnimet software.
- 15 Surface metrology guide website <http://www.predev.com/smg/standards.htm>; Last visited: 02/02/07.